

Localization and topological transitions in generalized non-Hermitian SSH models

X. Q. Sun^{1,1} and C. S. Liu^{1,1,*}

¹*Hebei Key Laboratory of Microstructural Material Physics,
School of Science, Yanshan University, Qinhuangdao, 066004, China.*

(Dated: March 23, 2023)

We study the localization and topological transitions of the generalized non-Hermitian SSH models, where the non-Hermiticities are introduced by the complex quasiperiodic hopping and the nonreciprocal hopping. We elucidate the universality of the models and how many models can be mapped to them. Under the open boundary condition, two delocalization transitions are found due to the competition between the Anderson localization and the boundary localization from the nontrivial edge states and the non-Hermitian skin effect. Under the periodic boundary condition, only one delocalization transition is found due to the disappearance of the non-Hermitian skin effect. The winding numbers of energy and the Lyapunov exponents in analytical form are obtained to exactly characterize the two delocalization transitions. It finds that the delocalization transitions don't accompany the topological transition. Furthermore, the large on-site non-Hermiticity and the large nonreciprocal hopping are all detrimental to the topological transitions. However, the large nonreciprocal hopping enhances the Anderson localizations. The above analyses are verified by calculating the energy gap and the inverse of the participation ratio numerically.

I. INTRODUCTION

As the topological edge states are protected by the symmetry, the topological phases are expected to be immune to the perturbations of disorders [1–3]. Nevertheless, the strong disorders induce the destructive interference of scattered waves and lead to the localization of all the states [4, 5]. The presence of the Anderson localized phase accompanies the disappearance of the topological nontrivial phase. The disorders connect the two unrelated quantum states which give rise to the topological Anderson insulators [6–8]. Recently, the ability to engineer non-Hermitian Hamiltonians and the related observations of unconventional topological edge modes attract a great interest to extend the topological band theory to non-Hermitian systems [9]. The interplays between the topology and non-Hermiticity result in a plethora of exotic phenomena that have no Hermitian counterparts, e.g., the Weyl exceptional ring [10], the point gap [11]. In particular, the realization of the nonreciprocal hopping induces the non-Hermitian skin effect. Comparing to the Hermitian case where the zero-energy states are localized at the boundary only, the non-Hermitian skin effect results in the asymmetrical localization where not only the nontrivial edge states, but also all the trivial states are localized at the boundary. The competition of the boundary localization and bulk localization must lead to the delocalization transitions. In the presence of the non-Hermitian skin effect, a characteristic signature is the breakdown of the conventional bulk-boundary correspondence [9, 12–27]. The question arises as to whether or not the delocalization transitions accompany the topological transitions. Where are the phase boundaries and how the non-Hermitian skin effect modifies the phase transitions?

The Anderson localizations are generally studied with the Aubry-André-Harper (AAH) model which is the periodic lattice modulated by quasiperiodic potential. Quasicrystals constitute an intermediate phase between fully periodic lattices and fully disordered media, showing a long-range order without periodicity [28, 29]. This solves the problems of reliably controlling disorders in solid-state systems where the Anderson localization could only be studied indirectly or through numerical simulations. As the AAH model can be mapped to the lattice version of the two-dimensional integer Hall effect problem, it gives the opportunity to study the Anderson localization and topological properties simultaneously [30, 31]. The exact localization-delocalization transition can be obtained by the duality transformation between real and momentum spaces [32–42].

When the non-Hermiticities are further introduced to the AAH model by the complex on-site quasiperiodic potentials, it was found that the self-dual symmetry still determines the transitions from topological nontrivial phase to localized phase [43–48]. The quantum phase transitions still have the topological nature characterized by the winding numbers. However, when the non-Hermiticity is from nonreciprocal hopping, the induced non-Hermitian skin effect leads to the asymmetric localized states [45, 47, 48]. It finds that the Anderson localization is not necessarily in accordance with the topological phase transitions. A dip is found in the quasiperiodic potential dependence of the averaged inverse participation ratios which indicates the delocalization transition [45]. The transition point can be exactly proved by the skin effect rescaling.

Up to now, the studies of the non-Hermitian topological Anderson transitions mainly focus on the AAH models [38, 44, 45, 48, 49]. The Su-Schrieffer-Heeger (SSH) model for polyacetylene is the simplest one-dimensional topological insulator with the chirality symmetry [50]. As many non-Hermitian models can be mapped to var-

* cslu@ysu.edu.cn

ious non-Hermitian versions of the extended SSH models [27], they have become the typical models to study the non-Hermitian effects. In particular, in the presence of the non-Hermitian skin effect due to the nonreciprocal hopping, the generalized Brillouin zone of the non-Hermitian SSH model is proposed to recover the bulk-boundary correspondence [12–27]. The influence of the non-Hermitian skin effect on disordered SSH model is explored and the result shows that the non-Hermiticity can enhance the topological phase against disorders by increasing bulk gaps [51]. The onset of a mobility edge and the topological phase transition in the disordered SSH chain connected to two external baths was investigated the Lindblad equation method [52]. The localization/delocalization of the disordered chain can be recovered by the scaling properties of the nonequilibrium stationary current. However, the winding numbers and Lyapunov exponents in analytical forms are still lacking to characterize the relationship between the topological transitions and Anderson transitions.

In this paper, we study the non-Hermitian generalized SSH model, where the non-Hermiticities are introduced by both the complex quasiperiodic modulation hopping and the nonreciprocal hopping. The main results of this article include the following: (i) We find the equivalence and the universality of the models connected by the similarity transformation. (ii) The winding numbers and the Lyapunov exponents in analytic form are obtained to characterize the topological transition and localization transition. (iii) We clarify the origin of the two delocalization transitions. (iv) The influences of non-Hermiticities on the localizations and topological phase transitions are given.

The rest of paper is organized as follows: In Sec. II we present the Hamiltonian of the generalized non-Hermitian SSH model and its various equivalent models. We explain the equivalence of the hopping terms and elucidate why the complex quasiperiodic modulation hopping can be applied in any of the terms. We also clarify how the nonreciprocal hopping can be transformed from one form to another by the similarity transformations. The winding numbers and the Lyapunov exponents are derived in Sec. III to characterize the topological transition and the Anderson transition. In Sec. IV, the phase diagram of the model is obtained by calculating the inverse of participation ratio. A brief summary is presented in Sec. V.

II. MODEL

We consider the non-Hermitian SSH model [pictorially shown in Fig. 1 (a)] [50, 53, 54]. The Hamiltonian is described by

$$H = \Psi^\dagger h \Psi = \sum_n [t_{1,n} a_n^\dagger b_n + t_{1,n} b_n^\dagger a_n + (t_2 - \gamma_2) a_{n+1}^\dagger b_n + (t_2 + \gamma_2) b_n^\dagger a_{n+1}] \quad (1)$$

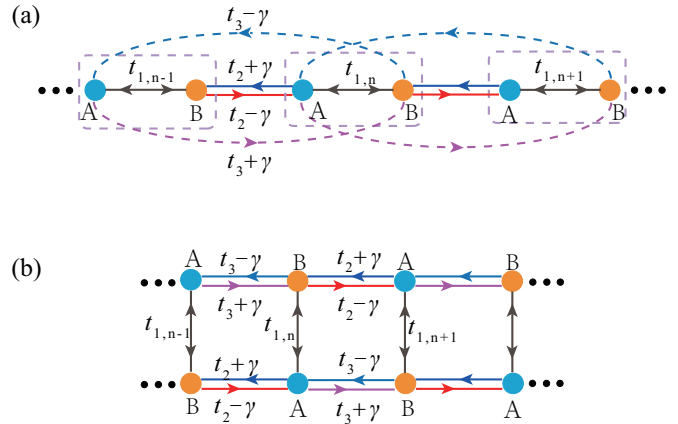


FIG. 1. (a) Non-Hermitian SSH model and (b) its equivalent two-leg ladder model.

$$+ (t_3 - \gamma_3) a_n^\dagger b_{n+1} + (t_3 + \gamma_3) b_{n+1}^\dagger a_n],$$

where Nambu operator $\Psi^\dagger = (a_1^\dagger, b_1^\dagger, \dots, a_L^\dagger, b_L^\dagger)$. a_n^\dagger and b_n^\dagger (a_n and b_n) are the creation (annihilation) operators of a spinless fermion at lattice site n . $t_{1,n}$, t_2 and t_3 are the hopping amplitudes. The parameters γ_2 and γ_3 induce the asymmetric coupling. The model in Eq. (1) has chiral symmetry $\mathcal{S}h\mathcal{S}^{-1} = -h$, with operator $\mathcal{S} = \text{diag}(1, -1, \dots, 1, -1, \dots)$. The chiral symmetry ensures the eigenvalues ($E, -E$) pairs.

The hopping amplitude $t_{1,n}$ is set to be site dependent, i.e.

$$t_{1,n} = 2V \cos(2\pi\beta n + i\alpha), \quad (2)$$

with the strength V . α depicts the non-Hermiticity of the quasiperiodic hopping. β is an irrational number which is used to characterize the quasiperiodicity. The irrational number is usually taken by the value of the inverse of golden ratio [$\beta = (\sqrt{5} - 1)/2$] which in practice approximated by rational numbers $\beta = F_n/F_{n+1}$ with the n th Fibonacci number F_n . The n th Fibonacci number $F_n = F_{n-1} + F_{n-2}$ and the 1th and 2th Fibonacci numbers are assumed to be $F_1 = 1$ and $F_2 = 1$ respectively. In numerical simulations, a finite (yet arbitrarily large) number of lattice sites $L = F_{n+1}$ is assumed usually to eliminate the domain wall of the PBC and to reduce the finite-size effects. The quasiperiodic term $t_{1,n}$ acts as the disorders and induces localizations of the states.

It should be emphasized that $t_{1,n}$, t_2 and t_3 are equivalent and the quasiperiodicity can be set to any of the terms. The reason is the model in Fig. 1 (a) is equivalent to the two-leg ladder model [pictorially shown in Fig. 1 (b)]. Exchanging $t_{1,n}$ and t_2 terms, the AB lattice of the model becomes merely the BA lattice which corresponds to relabeling $b_n \rightarrow b_{n+1}$. Similarly, the model remains unchanged when exchanging t_2 and t_3 terms.

The introduction of parameters γ_2 and γ_3 do not lose the universality since the asymmetry of hopping $t_2 \pm \gamma_2 = \tau_{\pm} = \bar{t}_2 e^{\pm \phi_2}$ and $t_3 \pm \gamma_3 = \bar{t}_3 e^{\pm \phi_3}$ can be shifted from one term to another with the similarity transformations under the open boundary condition (OBC) [27]. After the similarity transformations, we obtain the equivalent models. For example, under the OBC, the Hamiltonian of this model in Eq. (1) can be transformed into

$$\begin{aligned} \hat{H} = \hat{\Psi}^\dagger \hat{h} \hat{\Psi} = \sum_n & \left[t_{1,n} \hat{a}_n^\dagger \hat{b}_n + t_{1,n} \hat{b}_n^\dagger \hat{a}_n \right. \\ & + (t_2 - \gamma_2) r_1^{-1} \hat{a}_{n+1}^\dagger \hat{b}_n + (t_2 + \gamma_2) r_1 \hat{b}_n^\dagger \hat{a}_{n+1} \\ & \left. + (t_3 - \gamma_3) r_1 \hat{a}_n^\dagger \hat{b}_{n+1} + (t_3 + \gamma_3) r_1^{-1} \hat{b}_{n+1}^\dagger \hat{a}_n \right], \end{aligned} \quad (3)$$

by the similarity transformation $\hat{h} = S_1^{-1} h S_1$ and $\hat{\Psi} = S_1^{-1} \Psi$ with

$$S_1 = \text{diag}\{r_1, r_1, r_1^2, r_1^2, \dots, r_1^{L/2}, r_1^{L/2}\}. \quad (4)$$

When $r_1 = e^{\phi_3}$, the non-Hermiticity in t_3 term is killed and the non-Hermiticity is transformed into t_2 term completely. However, when $r_1 = e^{-\phi_2}$, the non-Hermiticity in t_2 term is eliminated and the non-Hermiticity remains in t_3 term. In such case $r_1 = e^{-\phi_2}$, further doing the transformation $\check{h} = S_2^{-1} \hat{h} S_2$ and $\check{\Psi} = S_2^{-1} \hat{\Psi}$ with

$$S_2 = \text{diag}\{1, r_2, r_2, r_2^2, r_2^2, \dots, r_2^{L/2-1}, r_2^{L/2-1}, r_2^{L/2}\}, \quad (5)$$

and $r_2 = e^{-(\phi_2 + \phi_3)/2}$, the model in Eq. (3) becomes

$$\begin{aligned} \check{H} = \check{\Psi}^\dagger \check{h} \check{\Psi} = \sum_n & \left[t_{1,n} r_2^{-1} \check{a}_n^\dagger \check{b}_n + t_{1,n} r_2 \check{b}_n^\dagger \check{a}_n \right. \\ & \left. + \bar{t}_2 \check{a}_{n+1}^\dagger \check{b}_n + \bar{t}_2 \check{b}_n^\dagger \check{a}_{n+1} + \bar{t}_3 \check{a}_n^\dagger \check{b}_{n+1} + \bar{t}_3 \check{b}_{n+1}^\dagger \check{a}_n \right]. \end{aligned} \quad (6)$$

The non-Hermiticity in t_3 term is transformed into t_1 term.

It is easy to define the unity operator U which transforms the Numb creation operator Ψ^\dagger in Eq. (1) to

$$\begin{aligned} \Phi^\dagger = \Psi^\dagger U & = \left(a_1^\dagger, b_1^\dagger, \dots, a_L^\dagger, b_L^\dagger \right) U \\ & = \left(a_1^\dagger, a_2^\dagger, \dots, a_L^\dagger, -ib_1^\dagger, -ib_2^\dagger, \dots, -ib_L^\dagger \right) \\ & = \left(u^\dagger, v^\dagger \right). \end{aligned}$$

With the unity operator U , the Hamiltonian h in Eq. (1) under the PBC can be transformed into two block off-diagonal form

$$\tilde{h} = U^\dagger h U = -i\tilde{h}_+ \sigma_+ + i\tilde{h}_- \sigma_- \quad (7)$$

here

$$\tilde{h}_+ = \begin{pmatrix} t_{1,n} & t_3 - \gamma_3 & & t_2 - \gamma_2 \\ t_2 - \gamma_2 & t_{1,n} & & \ddots \\ & & \ddots & t_{1,n} & t_3 - \gamma_3 \\ t_3 - \gamma_3 & & t_2 - \gamma_2 & t_{1,n} \end{pmatrix},$$

$$\tilde{h}_- = \begin{pmatrix} t_{1,n} & t_2 + \gamma_2 & & t_3 + \gamma_3 \\ t_3 + \gamma_3 & t_{1,n} & & \ddots \\ & & \ddots & t_{1,n} & t_2 + \gamma_2 \\ t_2 + \gamma_2 & & t_3 + \gamma_3 & t_{1,n} \end{pmatrix}$$

and $\sigma_{\pm} = (\sigma_x \pm i\sigma_y)/2$. Under the OBC, there aren't non-diagonal elements in the matrix \tilde{h}_+ and \tilde{h}_- . In the new Numb operator Φ , the Hamiltonian in Eq. (1) becomes $H = \Phi^\dagger \tilde{h} \Phi$ and the eigenfunction is given by $\tilde{h} \Phi = E_n \Phi$.

With the block off-diagonal form, the eigenvalue problem turns into

$$\begin{aligned} -i\tilde{h}_+ v_n & = E_n u_n, \\ i\tilde{h}_- u_n & = E_n v_n. \end{aligned}$$

We then obtain

$$\begin{aligned} \tilde{h}_+ \tilde{h}_- u_n & = E_n^2 u_n, \\ \tilde{h}_- \tilde{h}_+ v_n & = E_n^2 v_n. \end{aligned} \quad (8)$$

u_n and v_n can be treated as the single-particle states, and have the same properties. We find the zero-energy states by solving the Eq. (8). The merit is the dimension of $\tilde{h}_+ \tilde{h}_-$ or $\tilde{h}_- \tilde{h}_+$ is equal to half of that of h in Eq. (1).

Replacing $t_2 \rightarrow -t - \Delta$, $t_3 \rightarrow -t + \Delta$, $\gamma_2 = \gamma_3 = \gamma$ and $t_{1,n} \rightarrow V_j$, the non-Hermitian SSH Hamiltonian in Eq. (7) is mapped to non-Hermitian AAH models with p-wave pairing [47]

$$\begin{aligned} H & = \sum_j \left[-(t + \gamma) c_j^\dagger c_{j+1} - (t - \gamma) c_{j+1}^\dagger c_j \right. \\ & \quad \left. + \Delta c_j c_{j+1} + \Delta c_{j+1}^\dagger c_j^\dagger \right] + \sum_j V_j c_j^\dagger c_j \\ & = \tilde{\Psi}_L^\dagger \tilde{h} \tilde{\Psi}_R, \end{aligned} \quad (9)$$

in the Majorana fermion representation. c_j^\dagger is the creation operator of a spinless fermion at lattice site j and t is the hopping amplitude and set as the unit energy ($t = 1$). Δ is the p-wave pairing amplitude. The Majorana fermion operator

$$\tilde{\Psi}_L^\dagger = (\nu_1^A, \nu_2^A \dots \nu_L^A, \nu_1^B, \nu_2^B \dots \nu_L^B),$$

where $\nu_j^A \equiv c_j + c_j^\dagger$ and $\nu_j^B \equiv i(c_j - c_j^\dagger)$ are operators of two Majorana fermions belonging to one physical site. They satisfy relations $(\nu_j^\kappa)^\dagger = \nu_j^\kappa$ and $\{\nu_j^\kappa, \nu_k^\lambda\} = 2\delta_{jk}\delta_{\kappa\lambda}$ ($\kappa, \lambda = A, B$) [55, 56]. In the case of $\gamma = 0$, localization and topological phase transitions of model (9) have been studied in Ref. [47].

III. THE TOPOLOGICAL TRANSITION AND THE ANDERSON TRANSITION

A. Winding number

Considering the periodicity of AB lattice and the modulated quasiperiodic potential, the topological transitions

can in principle be discussed in GBZ with the technique proposed in Ref. [12–26]. The topological transition can also be studied with its topological equivalent model in conventional BZ introduced in Ref. [27]. However, when the quasiperiodic potential in Eq. (2) is used to depict the disorder, a large order of Fibonacci number must be used to ensure the long term disorder which results in the complexity of the discussion. Alternatively, a phase δ is usually added in the complex quasiperiodic potential

$$V_j = 2V \cos(2\pi\beta j + i\alpha + \delta/L),$$

to introduce an additional dimension. The winding number of energy is often used to characterize the topological nontrivial phase and defined as

$$\nu = \lim_{L \rightarrow \infty} \oint \frac{d\delta}{2\pi i} \partial_\delta [\ln \det(H)],$$

here the Hamiltonian H is defined under the PBC [11]. ν can be used to depict how the complex spectral trajectory E encircles a base energy 0 in the complex energy plane, when δ changes from 0 to 2π .

With the block off-diagonal Hamiltonian in Eq. (7), the winding number is given by [57, 58]

$$\nu = \lim_{L \rightarrow \infty} \oint \frac{d\delta}{2\pi i} \partial_\delta [\ln \det(\tilde{h}_+ \tilde{h}_-)],$$

which is the summation of winding numbers of winding vectors $\det(\tilde{h}_+)$ and $\det(\tilde{h}_-)$ in the complex energy plane. In the large limit $L \rightarrow \infty$, $\det(\tilde{h}_+)$ and $\det(\tilde{h}_-)$ have the analytical forms which are given by

$$\det(\tilde{h}_\pm) = -\tau_\pm^L + (-1)^{L+1} V^L e^{L\alpha - i\delta} + P_\pm, \quad (10)$$

where

$$\tau_\pm = \max(\bar{t}_2 e^{\pm\phi_2}, \bar{t}_3 e^{\pm\phi_3}), \quad (11)$$

and $P_\pm = [\max(\bar{t}_2 \bar{t}_3 e^{\pm(\phi_2 + \phi_3)}, V)]^L$. The detailed calculations can consult the Refs [45, 47, 56, 59]. P_\pm can be neglected under the PBC. The winding number is given by $\nu = \nu_+ + \nu_-$,

$$\nu_\pm = \Theta(Ve^\alpha - \tau_\pm), \quad (12)$$

here $\Theta(x)$ is the step function. The topological transition points are given by $V_{T,\pm} = \tau_\pm e^{-\alpha}$ which indicates that the onsite non-Hermiticity α is always negative correlation with topological transition. Without losing the generality, it assumes that $\bar{t}_2 e^{\phi_2} > \bar{t}_3 e^{\phi_3}$ and $\bar{t}_2 e^{-\phi_2} > \bar{t}_3 e^{-\phi_3}$. We get the parameter $\tau_\pm = \bar{t}_2 e^{\pm\phi_2} = t_2 \pm \gamma_2$. With increasing the disorder intensity V , the nontrivial edge state is destroyed when $V = \tau_- e^{-\alpha}$. Further increasing the disorder intensity V , the system is still in the trivial topological phase. So the topological transition point is $V_T = \tau_- e^{-\alpha}$ which indicates that the nonreciprocal parameter γ_2 is negative correlation with topological transition.

B. Lyapunov exponent

Under the weak disorder perturbations, the energy-band structure remains unchanged. For the topological nontrivial Hermitian system, the nontrivial edge states are almost localized at several sites while all the trivial states are Bloch waves and extend in the bulk. In such case, the localization is boundary localization which is from the nontrivial edge states. In the strong disorder case however, the energy-band structure is broken. The localization is determined by Anderson localization where all the states localize in the bulk. The nonreciprocal hopping induces the non-Hermitian skin effect and the asymmetrical (boundary) localization. The strong disorders also break the asymmetrical localization and lead to the Anderson localization. Accompanying the transition from boundary to Anderson localization, a delocalization must occur.

The transition from extended to localized phases can be clarified by the Lyapunov exponent η which is the inverse of localization length. In the localized phase, the wave function is exponentially decayed in the localization center n_0 , i.e. $\exp(-\eta|n - n_0|)$. Concerning various localizations, four kinds of the Lyapunov exponents are needed to depict the localizations of the model.

The first Lyapunov exponent is related to the nontrivial topological state whose definition is based on the transfer matrix approach [60]. If the system under OBC hosts a topological nontrivial state, the block off-diagonal Hamiltonian in Eq. (7) has the zero-energy mode which should satisfy $\tilde{h}_+ v_n = 0$. In transfer matrix form, the equation can be rewritten as

$$\begin{pmatrix} v_{j+1} \\ v_j \end{pmatrix} = T_j \begin{pmatrix} v_j \\ v_{j-1} \end{pmatrix},$$

with

$$T_j = \begin{pmatrix} -\frac{V_j}{t_3 - \gamma_3} & -\frac{t_2 - \gamma_2}{t_3 - \gamma_3} \\ 1 & 0 \end{pmatrix}.$$

The transfer matrix of the whole system is given by $T = \prod_{j=1}^L T_j$ with the two eigenvalues λ_1 and λ_2 . Supposing $|\lambda_1| < |\lambda_2|$, the Lyapunov exponent of the edge states is defined as

$$\eta_1 = -\lim_{L \rightarrow \infty} \frac{\ln|\lambda_2|}{L}. \quad (13)$$

In order to determine η_1 , we perform a similarity transformation $ST_j S^{-1} = \xi^{-1/2} \tilde{T}_j$ with $S = \text{diag}(\xi^{1/4}, \xi^{-1/4})$ and

$$\xi = \frac{t_3 - \gamma_3}{t_2 - \gamma_2}.$$

After the similarity transformation, the transfer matrix T_j of the non-Hermitian AB model modulated by disorder is transformed into

$$\tilde{T}_j = \begin{pmatrix} \frac{V_j \sqrt{\xi}}{t_3 - \gamma_3} & 1 \\ 1 & 0 \end{pmatrix},$$

which is a transfer matrix of the Hermitian AA lattice. However, the non-Hermiticity and nontrivial topological properties of the model are transformed into the disorder term and an extra parameter $\xi^{-1/2}$. The transfer matrix of the whole system is given by $T = \prod_{j=1}^L T_j = \xi^{-L/2} \prod_{j=1}^L \tilde{T}_j = \xi^{-L/2} \tilde{T}$. Due to the deficiency of the edge state in the Hermitian AA lattice, the Lyapunov exponent of the model corresponding to the transfer matrix \tilde{T}_j is zero obviously which lead to the Lyapunov exponent of the edge state $\eta_1 = \ln \xi^{-1/2}$ from the Eq. (13).

The second Lyapunov exponent concerns the Anderson localization of all the states. According to the Thouless mechanism, the Lyapunov exponent of the Anderson localized state in the neighborhood of E_B can be computed as [61]

$$\eta_2 = \int d\varepsilon \rho(\varepsilon) [\ln |\varepsilon - E_B| - \ln(\epsilon_+) - \ln(\epsilon_-)],$$

where $\rho(\varepsilon)$ is the density of state. The parameters ϵ_+ and ϵ_- are introduced to reset the energy scale. E_B is set to be 0 for the sake of simplicity since η_2 is energy-independent according to numerical analysis. η_2 is used to characterize the bulk localization. The following derivations of η_2 of the model are based on the Ref. [59]. Under the OBC, we therefore obtain the Lyapunov exponent $\eta_{2,\pm} = \ln \frac{Ve^\alpha}{\epsilon_\pm}$ where $\epsilon_\pm = \sqrt{(t_2 \pm \gamma_2)(t_3 \pm \gamma_3)}$. Since the log function needs $Ve^\alpha > \epsilon_\pm$, we can get two localization transition points $V_{L,\pm} = e^{-\alpha} \epsilon_\pm$. $\eta_{2,+}$ is meaningless since the system has been in Anderson localization phase when $V > V_{L,-} = e^{-\alpha} \epsilon_-$. When $V > V_{L,+} = e^{-\alpha} \epsilon_+$, the large quasiperiodic intensity modifies the decay exponent of the Anderson localized state according the formulae $\exp(-\eta |n - n_0|)$. So the Lyapunov exponent is given by $\eta_{2,-} = e^{-\alpha} \epsilon_-$ which indicates that the onsite non-Hermiticity α and the nonreciprocal parameters (γ_2, γ_3) are all negative correlation with the Anderson transition.

When the localization of the nontrivial topological state is further modulated by the Anderson localization of all the states, it gives the third Lyapunov exponent. Combining the boundary localization of the nontrivial state and bulk localization, the Lyapunov exponent is given by

$$\eta = \eta_{2,-} - \eta_1 = \ln(Ve^\alpha - \tau_-). \quad (14)$$

As a result, the transition point of the nontrivial topological state is $V = e^{-\alpha} \tau_-$ which equals to the topological transition point $V_{T,-}$.

Under the PBC, the non-Hermitian skin effect vanishes even in the presence of the nonreciprocal hopping. In the absence of the asymmetrical localization, the calculation of Lyapunov exponent can consult the Ref. [47]. We can obtain two values of the fourth Lyapunov exponent $\eta_\pm = \ln \frac{Ve^\alpha}{\tau_\pm}$ which are the same as the winding numbers. Since the log function needs $Ve^\alpha > \tau_\pm$, we can get two localization transition points $V = e^{-\alpha} \tau_\pm$ which are just the topological transition points $V_{T,\pm}$.

IV. PHASE DIAGRAM

With the topological transition points $V_{T,\pm}$ and the Anderson transition points $V_{L,\pm}$ in analysis forms, we are ready to concretely discuss the two kinds of transitions and their relations of the model. It is no different that whether the inverse of the golden ratio or rational numbers F_n/F_{n+1} is taken to be as β . When discussing the topological Anderson insulator under the OBC, the nontrivial zero-edge states are protected by the symmetry and the Anderson localized states determined by the disorder intensity, provided L is long enough. Under the PBC, the domain wall forms when bending the chain into a ring. The domain states are protected by the symmetry and can be characterized by the winding number [27, 62]. In particular, the Anderson localized states are from all the states of the ring and the contribution of the domain states is negligible. In addition, an open boundary can be taken as a special domain wall. As we know, the periodic boundary spectra can be well approximated by the open boundary spectra [26, 27]. The argument also supports the fact that we can obtain the same conclusion under two boundary conditions. As the result, we take the quasiperiodic parameter to be $\beta = (\sqrt{5} - 1)/2$ directly in numerical analysis. The metric is the chain limitation $L = F_{n+1}$ can be discarded.

The OBC spectra shown in Fig. 2 (a₁) and PBC spectra in Fig. (b₁) respectively. In the numerical analysis, t_2 is set to be a unit parameter and other parameters are $t_3 = 0.8$, $\alpha = 0.4$ and $\gamma_2 = \gamma_3 = \gamma = 1/3$. Comparing the two energy spectra, the zero-energy states are found in the OBC and PBC chains. To estimate the topological phase transitions, we plot semilog of the lowest $|E_n^2|$ of the two spectra in Fig. 2 (a₂) and (b₂) under the two kinds of boundary conditions. It finds that the open/close of the gap in Fig. 2 (b₂) is accompanied by the emerging of zero-energy in Fig. 2 (a₂). Hence, the dip of the energy in Fig. 2 (b₂) can be taken as an indicator to characterize the topological phase transition of the model. The first transition point in Fig. 2 (a₁) is consistent with the prediction by the formula $V_{T,-} = \tau_- e^{-\alpha} = (t_2 - \gamma) e^{-\alpha} = 0.4469$. However, the second transition point $V_{T,+} = \tau_+ e^{-\alpha} = (t_2 + \gamma) e^{-\alpha} = 0.8938$ don't accompany the gap closing of the OBC spectra in Fig. 2 (a₁), and the small dip appears in the PBC energy spectra in Fig. 2 (b₂). As previously pointed out, with increasing the disorder intensity V across $V_{T,-}$, the nontrivial edge state is destroyed. Further increasing the disorder intensity V across $V_{T,+}$, the system has been in the topological trivial phase. As a result, the topological transition point is $V_{T,-}$. We will see that the dip near $V_{T,+}$ is related to the Anderson transition.

We calculate the lattice length L dependence of two transition points in Fig. 2 (c) under the two kinds of boundary conditions. It finds that the topological transition approaches $V_{T,-} = \tau_- e^{-\alpha}$ under the OBC when L is larger than 900. Under the PBC however, the chain length $L > 500$ is enough to ensure the calculation ac-

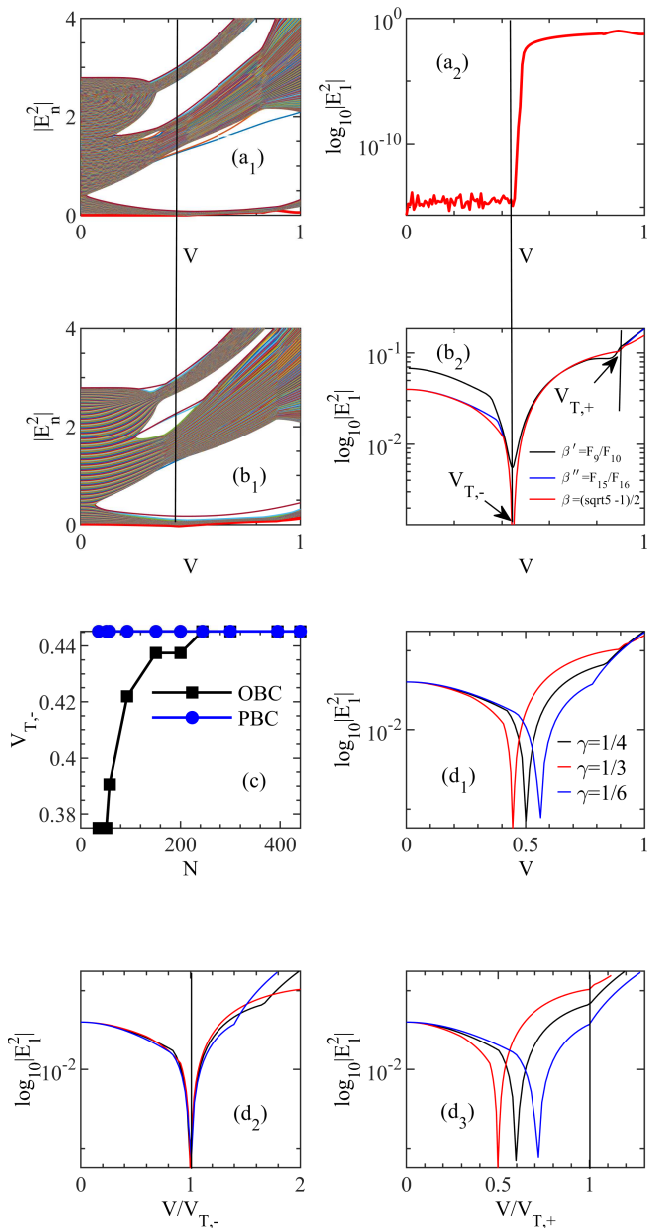


FIG. 2. Absolute values of spectra $|E_n^2|$ versus V for the non-Hermitian SSH model in Eq. (8) under the OBC (a₁) and the PBC (b₁). The parameters are taken to be $t_2 = 1$, $t_3 = 0.8$, $\alpha = 0.4$ and $\gamma = 1/3$. The lattice length is taken to be $L = 1200$. (a₂) The semilog of the lowest values of $|E_n^2|$ in (a₁). (b₂) The semilog plots of the lowest values of E_n under the PBC with different β and L . Black: $\beta = F_9/F_{10}$, $L = F_{10} = 55$. Blue: $\beta = F_{15}/F_{16}$, $L = F_{16} = 987$ and Red: $\beta = (\sqrt{5} - 1)/2$, $L = 1200$. (c) The finite-size analysis of the transition point $V_{T,-}$ under the OBC [black square solid line] and PBC [blue point solid line] (d₁) Semilog plots of the bulk energy gap of PBC spectra versus V with the different γ . Red: $\gamma = 1/3$, Blue: $\gamma = 1/6$ and Black: $\gamma = 1/4$. The other parameters remain unchanged. (d₂) Semilog plot of the bulk energy gap versus $V/V_{T,-}$. (d₃) Semilog plot of the bulk energy gap versus $V/V_{T,+}$.

curacy. So L is taken to be 1200 in all the numerical calculations. To verify the effectivity of the above numerical method, we also present the semilog plots of the lowest values of E_n under the PBC with different chain length: $L = F_{10} = 55$ [black line] and $L = F_{16} = 987$ [blue line] in Fig. 2 (b₂). Corresponding, β are taken to be F_9/F_{10} and F_{15}/F_{16} respectively. In the short lattice length $L = F_{10} = 55$ case, the error of the second transition point $V_{T,+}$ is obvious. With increasing the lattice length $L = F_{16} = 987$, all the two transition points are consistent with the case $\beta = (\sqrt{5} - 1)/2$ and $L = 1200$.

To further verify the topological transition of the model, we plot the semilog of the lowest $|E_n^2|$ of the PBC spectra in Fig. 2 (d₁) with different parameters. The amplitude of the quasiperiodic potential V is scaled by $V_{T,-}$ (d₂) and $V_{T,+}$ (d₃) respectively. The two dips collapse to the points which indicate the effectiveness of $V_{T,\pm} = \tau_{\pm} e^{-\alpha}$.

The inverse of the participation ratio

$$\text{IPR}_n = \sum_{m=1}^L |u_n(x_m)|^4$$

can be used to characterize the localization of a normalized state $u_n(x_m)$. For an extended state, IPR_n is of the order $1/L$, whereas it approaches to 1 for a localized state. When v_n is used to calculate IPR_n , the conclusions remain unchanged. the localization of the whole system can be characterized by the mean inverse of the participation ratio

$$\overline{\text{IPR}} = \sum_n \text{IPR}_n / L.$$

We calculate IPR_1 corresponding to the lowest $|E_n^2|$ shown in Fig. 3 (a) to understand the localization of the nontrivial topological phase. As a demonstration of the topological phase, we also plot the zero-energy number versus V in Fig. 3 (a). In the low V region near $V_{T,-} = e^{-\alpha}(t_2 - \gamma) = 0.4469$, a dip $V \approx 0.45$ dives in Fig. 3 (a). The appearance of the dip (de-localization) accompanying the topological transition is due to the localization competition between the nontrivial edge states and the disorders. The competition leads to the most extended case of the particle distributions (the smallest IPR_1) in the transition point. As expected, the zero-energy edge states [Fig. 3 (c₁) and (c₂)] indicate the system in the topological nontrivial phase when $V < V_{T,-}$. When $V > V_{T,-}$, the edge state (nontrivial topological phase) is breakdown. Further increasing $V > V_{T,+} = e^{-\alpha}(t_2 + \gamma) = 0.8938$, the edge state cannot exist. However, the other dip appears at $V = 0.89$ in Fig. 3 (a) and (b). As the result, the topological transition point is $V_{T,-} = e^{-\alpha}(t_2 - \gamma)$. The consistence of the above numerical result with the formulae $V_{T,-}$ verifies that the topological transition accompanies the breakdown of the zero-energy edge state, and the large non-Hermitian parameters α and γ are all detrimental to the topological transition.

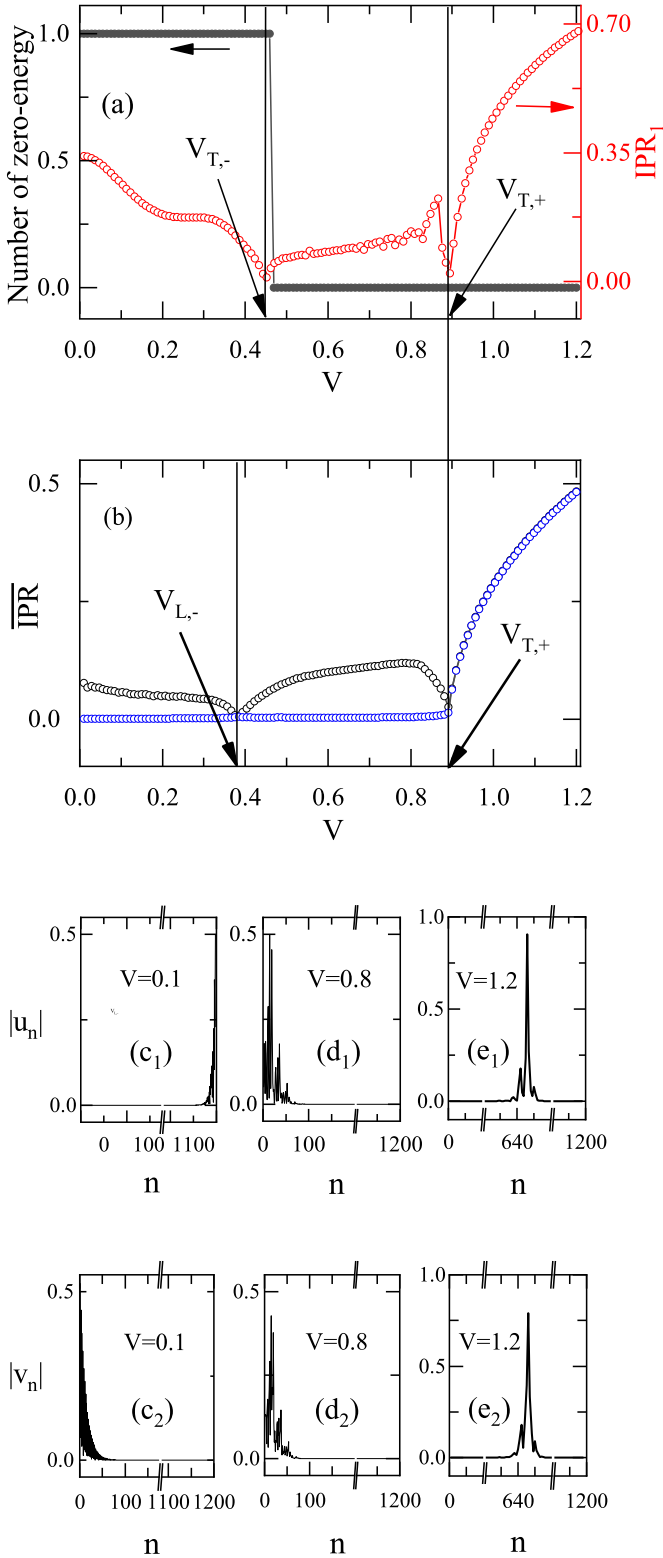


FIG. 3. Localization transitions. (a) $\overline{\text{IPR}}_1$ and number of zero-energy state versus V . (b) $\overline{\text{IPR}}$ of the state u versus V . The second row and the third row are the wave-function u_n and v_n of the lowest $|E_n^2|$ for the three different regions V under the OBC.

We calculate the averaged inverse participation ratios ($\overline{\text{IPR}}$) over the right eigenstates u_n in Eq. (8) under two kinds of boundary condition in Fig. 3 (b) to understand the Anderson localization. In the low V region near $V_{L,-} = e^{-\alpha}\epsilon_- = e^{-\alpha}\sqrt{(t_2 - \gamma)(t_3 - \gamma)} = 0.3739$, a deep $V \approx 0.38$ dives in Fig. 3 (b) under the OBC which is different from that in Fig. 3 (a). The appearance of the dip indicates the Anderson transition of the whole system doesn't accompany the topological transition which is contrast to the case of $\overline{\text{IPR}}_1$.

The inconsistency of the topological transition and Anderson transition can be understood as follow. When calculating $\overline{\text{IPR}}$, the contribution of edge zero-energy states is negligible. The delocalization transition is due to the localization competition between boundary localization of the bulk states from the non-Hermitian skin effect and the Anderson localization from the disorders. It is that non-Hermitian skin effect leads to all the states to localize at the boundary. In the absence of the non-Hermitian skin effect, all the bulk states are Bloch waves and the nontrivial topological states localize at the boundary. The boundary localization is determined by the nontrivial topological states only, which the Anderson transition accompanies the topological transition. $V_{T,-} > V_{L,-}$ also indicates that the topological edge states are protected by the symmetry, even in the non-Hermitian case, and the topological phases are expected to be immune to the perturbations of disorders.

Further increasing V ($> e^{-\alpha}\epsilon_+$), the system has been in the Anderson localization phase. We get the other transition point $V_{T,+} = e^{-\alpha}\tau_+ = 0.89$. Across the dip, $\overline{\text{IPR}}$ increases remarkably and the system in the Anderson localization phase shown in Fig. 3 (e₁) and (e₂). In the intermediate region, $V_{L,-} < V < V_{T,+}$, the spatial distribution of wave functions is shown in Fig. 3 (d₁) and (d₂). This transition also occurs under the PBC where $\overline{\text{IPR}}$ increases rapidly across the transition point [blue-circle in Fig. 3 (b)]. In such case, the non-Hermitian skin effect and zero-energy edge states disappear. Therefore, there isn't the boundary-localization nature. The Anderson localization is completely due to the disorders which lead to the destructive interference of scattered waves. The consistence of the second transition points in Fig. 3 (a) and (b) indicates the delocalizations have the same origin. Although it can be characterized by the winding number, the Anderson localization is unrelated to the topological transition. According to the formula $V_{T,+} = (t_2 + \gamma)e^{-\alpha}$, we conclude that the non-Hermitian skin effect enhances the Anderson localization.

V. SUMMARY

In summary, we have studied the localization and topological phase transitions of non-Hermitian SSH models, where the non-Hermiticities are introduced by the complex quasiperiodic hopping and the nonreciprocal hopping. In the presence of the nonreciprocal hopping, the

induced non-Hermitian skin effect leads to asymmetric localization of all the states. Under the OBC, increasing the intensity of the complex quasiperiodic hopping destroys the nontrivial zero-energy edge state and asymmetric localized states, and drives all the states into Anderson localized states. The competition between boundary localization and Anderson localization leads to the delocalization transitions. Due to the non-Hermitian skin effect, the localization transitions are not necessarily accompanied by the topological transitions. By analysing the winding number of energy and the Lyapunov exponent, we find the large nonreciprocal hopping is detrimental to the topological phase transitions, and enhances the Anderson localization. However, the large on-site non-Hermiticity is always detrimental to the Anderson local-

ization and topological phase transitions. Since the models have many topological equivalent models, the results we studied are useful for further studying the topological Anderson insulator experimentally.

ACKNOWLEDGMENTS

This work was supported by Hebei Provincial Natural Science Foundation of China (Grant No. A2012203174, No. A2015203387), Science and Technology Project of Hebei Education Department, China (Grant No. ZD2020200) and National Natural Science Foundation of China (Grant No. 10974169, No. 11304270).

-
- [1] Di Xiao, Ming-Che Chang, and Qian Niu, “Berry phase effects on electronic properties,” *Rev. Mod. Phys.* **82**, 1959–2007 (2010).
- [2] M. Z. Hasan and C. L. Kane, “Colloquium: Topological insulators,” *Rev. Mod. Phys.* **82**, 3045–3067 (2010).
- [3] Xiao-Liang Qi and Shou-Cheng Zhang, “Topological insulators and superconductors,” *Rev. Mod. Phys.* **83**, 1057–1110 (2011).
- [4] P. W. Anderson, “Absence of diffusion in certain random lattices,” *Phys. Rev.* **109**, 1492–1505 (1958).
- [5] Elihu Abrahams, *50 Years of Anderson Localization* (World Scientific, Singapore, 2010).
- [6] Jian Li, Rui-Lin Chu, J. K. Jain, and Shun-Qing Shen, “Topological anderson insulator,” *Phys. Rev. Lett.* **102**, 136806 (2009).
- [7] C. W. Groth, M. Wimmer, A. R. Akhmerov, J. Tworzydło, and C. W. J. Beenakker, “Theory of the topological anderson insulator,” *Phys. Rev. Lett.* **103**, 196805 (2009).
- [8] Hua Jiang, Lei Wang, Qing-feng Sun, and X. C. Xie, “Numerical study of the topological anderson insulator in hgte/cdte quantum wells,” *Phys. Rev. B* **80**, 165316 (2009).
- [9] Emil J. Bergholtz, Jan Carl Budich, and Flore K. Kunst, “Exceptional topology of non-hermitian systems,” *Rev. Mod. Phys.* **93**, 015005 (2021).
- [10] Yong Xu, Sheng-Tao Wang, and L.-M. Duan, “Weyl exceptional rings in a three-dimensional dissipative cold atomic gas,” *Phys. Rev. Lett.* **118**, 045701 (2017).
- [11] Zongping Gong, Yuto Ashida, Kohei Kawabata, Kazuaki Takasan, Sho Higashikawa, and Masahito Ueda, “Topological phases of non-hermitian systems,” *Phys. Rev. X* **8**, 031079 (2018).
- [12] V. M. Martinez Alvarez, J. E. Barrios Vargas, and L. E. F. Foa Torres, “Non-hermitian robust edge states in one dimension: Anomalous localization and eigenspace condensation at exceptional points,” *Phys. Rev. B* **97**, 121401 (2018).
- [13] Flore K. Kunst, Elisabet Edvardsson, Jan Carl Budich, and Emil J. Bergholtz, “Biorthogonal bulk-boundary correspondence in non-hermitian systems,” *Phys. Rev. Lett.* **121**, 026808 (2018).
- [14] Shunyu Yao and Zhong Wang, “Edge states and topological invariants of non-hermitian systems,” *Phys. Rev. Lett.* **121**, 086803 (2018).
- [15] Shunyu Yao, Fei Song, and Zhong Wang, “Non-hermitian chern bands,” *Phys. Rev. Lett.* **121**, 136802 (2018).
- [16] Kazuki Yokomizo and Shuichi Murakami, “Non-bloch band theory of non-hermitian systems,” *Phys. Rev. Lett.* **123**, 066404 (2019).
- [17] Fei Song, Shunyu Yao, and Zhong Wang, “Non-hermitian skin effect and chiral damping in open quantum systems,” *Phys. Rev. Lett.* **123**, 170401 (2019).
- [18] Ching Hua Lee and Ronny Thomale, “Anatomy of skin modes and topology in non-hermitian systems,” *Phys. Rev. B* **99**, 201103 (2019).
- [19] Fei Song, Shunyu Yao, and Zhong Wang, “Non-hermitian topological invariants in real space,” *Phys. Rev. Lett.* **123**, 246801 (2019).
- [20] Dan S. Borgnia, Alex Jura Kruchkov, and Robert-Jan Slager, “Non-hermitian boundary modes and topology,” *Phys. Rev. Lett.* **124**, 056802 (2020).
- [21] Kai Zhang, Zhesen Yang, and Chen Fang, “Correspondence between winding numbers and skin modes in non-hermitian systems,” *Phys. Rev. Lett.* **125**, 126402 (2020).
- [22] L. Jin and Z. Song, “Bulk-boundary correspondence in a non-hermitian system in one dimension with chiral inversion symmetry,” *Phys. Rev. B* **99**, 081103 (2019).
- [23] Qi-Bo Zeng, Yan-Bin Yang, and Yong Xu, “Topological phases in non-hermitian aubry-andré-harper models,” *Phys. Rev. B* **101**, 020201 (2020).
- [24] Ching Hua Lee, Linhu Li, Ronny Thomale, and Jiangbin Gong, “Unraveling non-hermitian pumping: Emergent spectral singularities and anomalous responses,” *Phys. Rev. B* **102**, 085151 (2020).
- [25] Yifei Yi and Zhesen Yang, “Non-hermitian skin modes induced by on-site dissipations and chiral tunneling effect,” *Phys. Rev. Lett.* **125**, 186802 (2020).
- [26] Zhesen Yang, Kai Zhang, Chen Fang, and Jiangping Hu, “Non-hermitian bulk-boundary correspondence and auxiliary generalized brillouin zone theory,” *Phys. Rev. Lett.* **125**, 226402 (2020).

- [27] Y. Z. Han, J. S. Liu, and C. S. Liu, “The topological counterparts of non-hermitian SSH models,” *New Journal of Physics* **23**, 123029 (2021).
- [28] S. Aubry and G. André, “Analyticity breaking and anderson localization in incommensurate lattices,” *Ann. Isr. Phys. Soc.* **3**, 133 (1980).
- [29] P. G. Harper, “Single band motion of conduction electrons in a uniform magnetic field,” *Proceedings of the Physical Society. Section A* **68**, 874–878 (1975).
- [30] Li-Jun Lang, Xiaoming Cai, and Shu Chen, “Edge states and topological phases in one-dimensional optical superlattices,” *Phys. Rev. Lett.* **108**, 220401 (2012).
- [31] Yaacov E. Kraus, Yoav Lahini, Zohar Ringel, Mor Verbin, and Oded Zilberberg, “Topological states and adiabatic pumping in quasicrystals,” *Phys. Rev. Lett.* **109**, 106402 (2012).
- [32] J. Biddle and S. Das Sarma, “Predicted mobility edges in one-dimensional incommensurate optical lattices: An exactly solvable model of anderson localization,” *Phys. Rev. Lett.* **104**, 070601 (2010).
- [33] J. Biddle, D. J. Priour, B. Wang, and S. Das Sarma, “Localization in one-dimensional lattices with non-nearest-neighbor hopping: Generalized anderson and aubry-andré models,” *Phys. Rev. B* **83**, 075105 (2011).
- [34] Sriram Ganeshan, J. H. Pixley, and S. Das Sarma, “Nearest neighbor tight binding models with an exact mobility edge in one dimension,” *Phys. Rev. Lett.* **114**, 146601 (2015).
- [35] Xiaopeng Li, J. H. Pixley, Dong-Ling Deng, Sriram Ganeshan, and S. Das Sarma, “Quantum nonergodicity and fermion localization in a system with a single-particle mobility edge,” *Phys. Rev. B* **93**, 184204 (2016).
- [36] Xiao Li, Xiaopeng Li, and S. Das Sarma, “Mobility edges in one-dimensional bichromatic incommensurate potentials,” *Phys. Rev. B* **96**, 085119 (2017).
- [37] Xiao Li and S. Das Sarma, “Mobility edge and intermediate phase in one-dimensional incommensurate lattice potentials,” *Phys. Rev. B* **101**, 064203 (2020).
- [38] Yanxia Liu, Yucheng Wang, Xiong-Jun Liu, Qi Zhou, and Shu Chen, “Exact mobility edges, \mathcal{PT} -symmetry breaking, and skin effect in one-dimensional non-hermitian quasicrystals,” *Phys. Rev. B* **103**, 014203 (2021).
- [39] X. Deng, S. Ray, S. Sinha, G. V. Shlyapnikov, and L. Santos, “One-dimensional quasicrystals with power-law hopping,” *Phys. Rev. Lett.* **123**, 025301 (2019).
- [40] Hepeng Yao, Alice Khoukli, Léa Bresque, and Laurent Sanchez-Palencia, “Critical behavior and fractality in shallow one-dimensional quasiperiodic potentials,” *Phys. Rev. Lett.* **123**, 070405 (2019).
- [41] Hepeng Yao, Thierry Giamarchi, and Laurent Sanchez-Palencia, “Lieb-liniger bosons in a shallow quasiperiodic potential: Bose glass phase and fractal mott lobes,” *Phys. Rev. Lett.* **125**, 060401 (2020).
- [42] Tong Liu, Xu Xia, Stefano Longhi, and Laurent Sanchez-Palencia, “Anomalous mobility edges in one-dimensional quasiperiodic models,” *SciPost Phys.* **12**, 027 (2022).
- [43] S. Longhi, “Topological phase transition in non-hermitian quasicrystals,” *Phys. Rev. Lett.* **122**, 237601 (2019).
- [44] Qi-Bo Zeng and Yong Xu, “Winding numbers and generalized mobility edges in non-hermitian systems,” *Phys. Rev. Research* **2**, 033052 (2020).
- [45] Hui Jiang, Li-Jun Lang, Chao Yang, Shi-Liang Zhu, and Shu Chen, “Interplay of non-hermitian skin effects and anderson localization in nonreciprocal quasiperiodic lattices,” *Phys. Rev. B* **100**, 054301 (2019).
- [46] Tong Liu, Hao Guo, Yong Pu, and Stefano Longhi, “Generalized aubry-andré self-duality and mobility edges in non-hermitian quasiperiodic lattices,” *Phys. Rev. B* **102**, 024205 (2020).
- [47] Xiaoming Cai, “Localization and topological phase transitions in non-hermitian aubry-andré-harper models with p -wave pairing,” *Phys. Rev. B* **103**, 214202 (2021).
- [48] Yanxia Liu, Qi Zhou, and Shu Chen, “Localization transition, spectrum structure, and winding numbers for one-dimensional non-hermitian quasicrystals,” *Phys. Rev. B* **104**, 024201 (2021).
- [49] Ling-Zhi Tang, Guo-Qing Zhang, Ling-Feng Zhang, and Dan-Wei Zhang, “Localization and topological transitions in non-hermitian quasiperiodic lattices,” *Phys. Rev. A* **103**, 033325 (2021).
- [50] W. P. Su, J. R. Schrieffer, and A. J. Heeger, “Solitons in polyacetylene,” *Phys. Rev. Lett.* **42**, 1698–1701 (1979).
- [51] Dan-Wei Zhang, Ling-Zhi Tang, Li-Jun Lang, Hui Yan, and Shi-Liang Zhu, “Non-hermitian topological anderson insulators,” *Science China Physics, Mechanics & Astronomy* **63**, 267062 (2020).
- [52] Andrea Nava, Gabriele Campagnano, Pasquale Sodano, and Domenico Giuliano, “Lindblad master equation approach to the topological phase transition in the disordered su-schrieffer-heeger model,” *arXiv e-prints*, arXiv:2210.10856 (2022).
- [53] H. C. Wu, X. M. Yang, L. Jin, and Z. Song, “Untying links through anti-parity-time-symmetric coupling,” *Phys. Rev. B* **102**, 161101 (2020).
- [54] Milad Jangjan and Mir Vahid Hosseini, “Floquet engineering of topological metal states and hybridization of edge states with bulk states in dimerized two-leg ladders,” *Scientific Reports* **10**, 14256 (2020).
- [55] A Yu Kitaev, “Unpaired majorana fermions in quantum wires,” *Physics-Uspekhi* **44**, 131–136 (2001).
- [56] Xiaoming Cai, Li-Jun Lang, Shu Chen, and Yupeng Wang, “Topological superconductor to anderson localization transition in one-dimensional incommensurate lattices,” *Phys. Rev. Lett.* **110**, 176403 (2013).
- [57] V. Gurarie, “Single-particle green’s functions and interacting topological insulators,” *Phys. Rev. B* **83**, 085426 (2011).
- [58] Zhong Wang and Shou-Cheng Zhang, “Topological invariants and ground-state wave functions of topological insulators on a torus,” *Phys. Rev. X* **4**, 011006 (2014).
- [59] Xiaoming Cai, “Boundary-dependent self-dualities, winding numbers, and asymmetrical localization in non-hermitian aperiodic one-dimensional models,” *Phys. Rev. B* **103**, 014201 (2021).
- [60] Wade DeGottardi, Manisha Thakurathi, Smitha Vishveshwara, and Diptiman Sen, “Majorana fermions in superconducting wires: Effects of long-range hopping, broken time-reversal symmetry, and potential landscapes,” *Phys. Rev. B* **88**, 165111 (2013).
- [61] D. J. Thouless, “A relation between the density of states and range of localization for one dimensional random systems,” *Journal of Physics C: Solid State Physics* **5**, 77–81 (1972).
- [62] Tian-Shu Deng and Wei Yi, “Non-bloch topological invariants in a non-hermitian domain wall system,”

